doi:10.3788/gzxb20134210.1231

基于马尔可夫随机场的红外有形目标检测算法

薛永宏[1,2],张涛[2],陈荣利[3],安玮[1],张寅生[2]

(1 国防科技大学 电子科学与工程学院,湖南 长沙 410073)

(2 北京跟踪与通信技术研究所,北京 100094)

(3 中国科学院西安光学精密机械研究所,西安 710119)

摘 要:构建了马尔可夫随机场自适应邻域系统,并将有形目标检测问题构建为马尔可夫随机场理论框架下背景与目标的二元分类问题.首先分析了影响目标形状的主要因素,归纳总结了典型的目标形状;其次以典型目标形状为模板构建了新的马尔可夫随机场邻域系统;然后构建了自适应邻域选择的代价函数,并基于有限差分算子创建了新的马尔可夫随机场势函数,进行背景与目标的分类判别.由于采用自适应邻域系统,所提算法在保持目标检测率的同时进一步降低了过门限率;比经典马尔可夫随机场邻域系统具有更好的目标形状保护新能.仿真试验结果表明,所提算法不仅具有较好的目标检测性能,而且可更好地保护目标形状的细节信息.

关键词:马尔可夫随机场;自适应邻域系统;有形目标检测;红外系统

中图分类号:TP391 **文献标识码**:A **文章编号**:1004-4213(2013)10-1231-7

Multi-shape Infrared Target Detection Algorithm Based on Markov Random Field

XUE Yong-hong[1,2], ZHANG Tao[2], CHEN Rong-li[3], AN Wei[1], ZHANG Yin-sheng[2]

(1 *College of Electronic Science and Engineering, National University of Defense Technology, Changsha, Hunan* 410073, *China*)

(2 *Beijing Institute of Tracking and Telecommunication Technology, Beijing* 100094, *China*)

(3 *Xi'an Institute of Optics and Precision Mechanics, Chinese Academy of Sciences, Xi'an* 710119, *China*)

Abstract: The problem of shape target detection was formulated as a binary classification problem of each pixel under Markov Random Field (MRF) theoretical framework and the adaptive neighborhood system of MRF was introduced. Firstly, the factors that cause the changing of target shapes were analyzed and classic target shapes presented on obtained infrared images were concluded. Secondly, the classic shapes were used as templates while establishing the new neighborhood system of MRF. Thirdly, to achieve the optimal detection performance, a criterion function for adaptively selecting the proper neighborhood for each pixel was proposed and at last a new potential function using finite difference operator was proposed for the classification of target and background at each pixel. For the usage of adaptive neighborhood system, the proposed algorithm has following advantages: further reduction of the threshold crossing rate of target detection in single image frame while maintaining the target detection rate and better preservation of target shape details than algorithms using classic neighborhood system of MRF. By simulations and experiments, the results show that the proposed algorithm can optimally detect targets under various image Signal-to-clutter ratios, and perfectly protect target shape details.

Foundation item: The National Natural Science Foundation of China (No. 61002022)

First author: XUE Yong-hong (1985—), male, Ph. D. degree candidate, mainly focuses on acquisition and processing of spatial information. Email: sanger_xue@126.com

Supervisor: AN Wei(1969—), female, professor, Ph. D. degree, mainly focuses on applications of integrated electronic warfare system and space information countermeasure. Email: nudtanwei@tom.com

Received: Jul. 3, 2013; **Accepted**: Aug. 8, 2013

Key words: Markov Random Field (MRF); Adaptive neighborhood system; Shape target detection; Infrared system

0 Introduction

Infrared surveillance system, for its perfect concealment performance, has been widely applied in defense and civilian sectors. The Space Based Infrared System (SBIRS) of USA government is one of the systems mainly built for detecting and tracking boost and midcourse ballistic missile targets[1]. Infrared target detection is one of the key technologies of SBIRS. Popularly used target detection algorithms can be divided into two categories, spatial filtering and time domain processing. The algorithms based on spatial filter mainly utilize the correlation between adjacent background pixels and the no correlation between target pixels and background pixels abutted against each other for target detection, while algorithms based on time domain processing primarily use the slowly varying characteristic of backgrounds and motion characteristic of targets. Algorithms based on time domain processing generally require images obtained at different time with high registration precision[2] and to get high registration precision, high stability of platform, accurate attitude measurements and numbers of landmarks used as control points are needed, but it is hard for SBIRS to satisfy the requirements.

To overcome this defect, an algorithm based on Markov Random Field (MRF) is introduced in this paper. MRF theory provides a convenient and consistent way for describing image pixels and features and the detection algorithm based on MRF can be classified as spatial filtering. For the long distance between SBIRS and their targets, most researchers assumed that targets in SBIRS were point targets and used point target model for detection[3]. But the existence of diffusion effect of optical systems broke this assumption. The diffusion of the radiant energy from point source makes sure that target in obtained images has shapes. The work in Ref. [4] introduced a pedestrian detection algorithm based on MRF. The algorithm considered the problem of pedestrian detection as the problem of image labeling of backgrounds and targets and used intensities of pedestrian targets to construct the posterior probability distribution function. To detect the small objects under sea background, the study in Ref. [5] proposed a sea target detection algorithm which applied the special and temporal correlation between neighbor pixels to construct the MRF's kernel function. Recent work in Ref. [6] experimented with adaptive morphological filter and introduced new MRF potential and energy function to detect the infrared small targets. Though the above studies can detect various targets under various complex backgrounds, the key shape details are neglected in above research works.

Since the shapes are helpful in accurately locating target, the main purpose of the work in this paper is detecting all the targets together with their complete shape details. The paper was arranged as following: the recent researches were summed in the first section. In the second section, the basic MRF theories that would use in the remainder of this paper were introduced, the factors that made the change of target shapes were analyzed and classic target shapes were concluded and used as templates while establishing the new MRF neighborhood system. Then a criterion function for adaptively selecting the proper neighborhood and a new MRF potential function was proposed for the classification of target and background. To prove the better performance of the proposed algorithm, simulations and experiments were made in the third section and the conclusion was given at the last.

1 Classic MRF model for target detection

Let $S=\{(i,j)\mid 1\leqslant i\leqslant M, 1\leqslant j\leqslant N\}$ be an image with $M\times N$ sites, M means the height of image and N means the width. $X=\{x_s\mid s\in S\}$ is a random field with a realization $x=\{x_{1,1},x_{1,2},\cdots,x_{M,N}\}$ that represents the gray values of the image. Let $\eta=\{\eta(s)\mid s\in S\}$ be the neighborhood system defined on S. The neighborhood system η describes the correlation between different sites. If and only if the random field X satisfies the following two conditions, it is said to be a Markov random field on S[7].

$$\begin{cases} P(X=x_s)\geqslant 0, \forall\, s\in S & \text{(Positivity)} \\ P(X=x_s\mid X=x_{S-\{s\}})= & \\ \quad P(X=x_s\mid X=x_{\eta(s)}), \forall\, s\in S) & \text{(Markovianity)} \end{cases} \tag{1}$$

where $S-\{s\}$ is the set difference, $x_{S-\{s\}}$ denotes the gray values at the sites in $S-\{s\}$.

The positivity is assumed for some technical

reasons and can usually be satisfied in practice. For example, when the positivity condition is satisfied, the joint probability $P(X=x_s)$ of any random field is uniquely determined by its local conditional probabilities[8]. The Markovianity depicts the local characteristics of X. Note that the definition of Markovianity does not imply that the neighbors of a site are necessarily close in terms of space distance, although it is assumed by many authors. According to the Hammersley-Clifford theorem, there is a mathematical equivalence between MRF and Gibbs Random Fields (GRF) distribution and this equivalence provides a tractable means of specifying the joint probability of MRF.

$$P(x_s|x_r, r\in\eta(s))=\frac{1}{Z}\exp\{-U(x_s)\}=\frac{1}{Z}\exp\{-\sum_{c\in C}V_c(x_s)\} \quad (2)$$

where $V_c(\cdot)$ is called potential function, $U(\cdot)$ is energy function and $Z=\sum_{x_s\in X}\exp\{-U(x_s)\}$ is normalizing constant called the partition function. c is a clique defined as a subset of sites in S and C is a set of all possible cliques.

The energy function $U(\cdot)$ usually describes the statistics of the gray difference between a pixel and pixels of its neighbors, the greater the difference is, the less likely the pixel and its neighbors are homogeneous and the smaller the joint probability of MRF becomes, or vice versa. To classify whether the pixel of current site is target or background, a judgment can be made according to the probability $P(x_s|x_r, r\in\eta(s))$ and a decision threshold T_d.

$$\begin{cases} x_s \text{ is target}, & \text{if } P(x_s|x_r, r\in\eta(s))<T_d \\ x_s \text{ is background}, & \text{if } P(x_s|x_r, r\in\eta(s))\geqslant T_d \end{cases} \quad (3)$$

To calculate the joint probability of an MRF, which is also a Gibbs distribution, it is necessary to evaluate the partition function Z. Because it is the sum over a combinatorial number of configurations in X, the computation is usually intractable. To circumvent the formidable difficulty therein, approximate technologies, such as maximum likelihood, pseudo-likelihood or Bayesian estimation, are often used in practice.

2 Markov random field with new neighborhood systems

2.1 Typical target shapes and new neighborhood system

Generally, target shapes presented in the obtained image have direct relation with the distribution of target energy. For the existence of diffusion effect in optical systems, radiant energy from point radiant source will form a spot on the focal plane and the radiant energy will be absorbed not only by one detector but also its neighbors, this phenomenon is naturally called point spread function (PSF) and can be expressed as

$$p_{(i_0,j_0)}(i,j)=\frac{1}{2\pi\sigma_{\text{psf}}^2}\exp\left(-\frac{(i-i_0)^2+(j-j_0)^2}{2\sigma_{\text{psf}}^2}\right) \quad (4)$$

where (i_0, j_0) is the position of target projection point under image coordinates, it has a consistent value. (i, j) is the image site of any other pixels, and gets its value in the set of integers. σ_{psf} is the standard deviation of the spread function.

It is clear that PSF has a formula of two-dimensional Gaussion distribution and the closer the position of projection point is to the center of the detector, the more concentrated the target energy is. If the projection point was located between two columns or rows, target energy will be absorbed by at least two detectors and target in the obtained image will have shapes but not a point that was always assumed by researchers in the past. Typical target shapes and their projection positions are shown in Fig. 1.

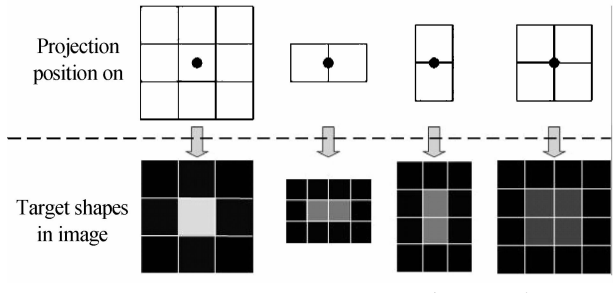

Fig. 1　Projection positions and typical target shapes

There are four different typical target shapes shown in Fig. 1: 1×1, 1×2, 2×1 and 2×2 shapes. For these shapes are helpful in distinguish the real target from false, these details must be protected while labeling/detecting. Recently, a popular way for detail preserving is using adaptive neighbor (AN) system[9]. According to the typical target shapes, the AN system at each site s can be formed as shown in Fig. 2.

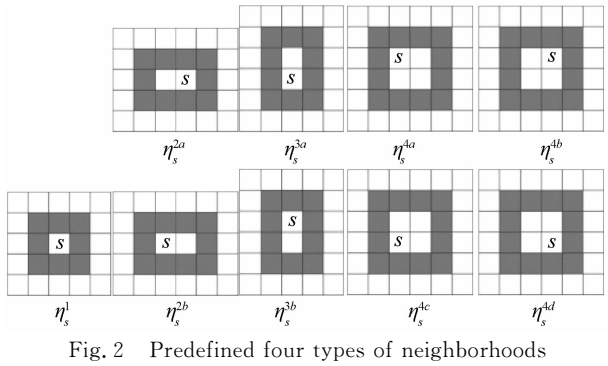

Fig. 2　Predefined four types of neighborhoods

The pixels with black color make up the neighborhood η_s^a of site s and the pixels with white color inner the black pixels form the target area $A_s^{(T)}$. Obviously, the site s is one of the pixels of the target area ($s \in A_s^{(T)}$). The configuration number of the neighborhood is different according to the pixel number inner the target area. For η_s^1 there is only one configuration at site s, but for η_s^2 and η_s^3 there are two configurations for each of them and for η_s^4 there are four. One of the objectives of this paper is to select a proper configuration for site s according to the observed image. The selected configuration must be a better characterization of the target area than other configurations in the neighborhood space.

2.2 Criterion function for neighborhood selection

Most researchers think that the selection of neighborhood is connected with the observation, because of the hidden property of MRF for image classification. In fact, choosing a suitable neighborhood system is a process of model selection. It is estimating a suitable neighborhood system through the observation, just like Forbes[10] estimating the class number based on the observation. Therefore, a term which characterizes observation should be used in choosing the suitable neighborhood.

Consider the example of Fig. 3. It shows the configuration of images in which there are two different targets with two different shapes. It is reasonable that η_s^1 in Fig. 2 should be selected as the neighborhood for the site s in Fig. 3(a) and η_s^{3b} should be selected for the site in Fig. 3(b). Then, the problem here is how to design a process to select the suitable neighborhood. In this section, the suitable neighborhood is selected through maximizing a criterion function.

The research in Ref. [11] shows that there are obvious differences between the energy distributions of target and background in infrared images. The energy distribution of target usually can be taken as a two dimensional pulse signal and that of the background is often considered as a two dimensional AR (Auto Regressive) process. So their energy distribution differences can be considered as the term which characterizes the observation and used in neighborhood selection. The term is formed from a finite difference operator which is introduced in Ref. [12] and in order to improve the applicability of the term, some researchers proposed that no prior knowledge other than the observed data should be used in constructing the operator. The operator is defined as following

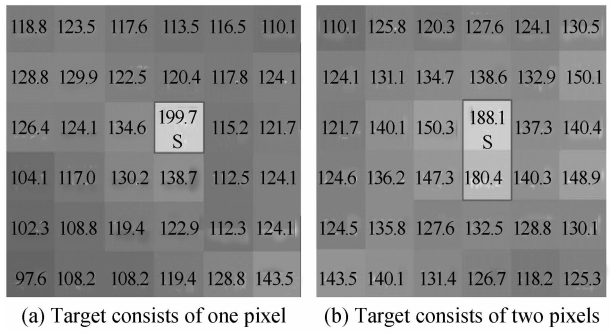

Fig. 3 Example of two subimages

$$d_{\eta_s^a}(x_s) = x_s - \frac{1}{|\eta_s^a|}\sum_{r\in\eta_s^a} x_r \tag{5}$$

where η_s^a is the adaptive neighborhood of site s, $|\eta_s^a|$ is its size and means the number of elements in η_s^a and x is the gray value of site s or r in the observed image. The most optimal configuration should be the one that maximizes the operator, namely

$$\tilde{\eta}_s^a = \underset{\eta_s^a}{\operatorname{argmax}}[d_{\eta_s^a}(x_s)] \tag{6}$$

In most cases, the Eqs. (5) and (6) can choose the just right neighborhood for site s. But it does not work well when the gray values of the backgrounds belong to a convex set. Still consider the two targets in Fig. 3(a) and (b) for example. The difference values calculated according to the Eq. (5) are shown in Table 1.

Table 1 The difference values of the predefined neighborhoods

Figure \ Neighborhood	η_s^1	η_s^2		η_s^3		η_s^4			
		(a)	(b)	(a)	(b)	(a)	(b)	(c)	(d)
Fig. 3(a)	75.71	76.87	75.04	77.79	78.92	76.85	**81.13**	77.54	78.32
Fig. 3(b)	42.87	46.21	41.71	48.58	51.07	49.58	**53.44**	46.86	51.15

Table 2 The difference values calculated by modified difference operator

Figure \ Neighborhood	η_s^1	η_s^2		η_s^3		η_s^4			
		(a)	(b)	(a)	(b)	(a)	(b)	(c)	(d)
Fig. 3(a)	**75.71**	11.77	−9.46	−1.51	17.92	−10.34	11.63	−6.97	−0.97
Fig. 3(b)	42.87	8.41	−9.09	−0.92	**43.37**	−1.22	12.64	−8.34	−2.25

The example data in Table 1 shows that the neighborhoods selected for the two targets are both η_s^{4b}, but not the behooved η_s^1 and η_s^{3b}. That is because x_s the gray value of site s cannot represents that of the whole target area $A_s^{(T)}$. Thus the difference operator defined above attends to choose neighborhoods with wider target area. To overcome this defect, a proper $\hat{x}_s$ that characterizes background when there is background pixels in target area and target when there is none. Through serious and careful analyses, a minimum operation is used here and the difference operator is modified as

$$\hat{d}_{\eta_s^a}(x_s)=\hat{x}_s-\frac{1}{|\eta_s^a|}\sum_{r\in\eta_s^a}x_r \tag{7}$$

where $\hat{x}_s=\min_{t\in A_s^{(T)}}(x_t)$. The difference values calculated by the modified operator are shown in table 2. It is noted that the modified operator selected the just right neighborhood and can perfectly deal with the defect.

2.3 New potential function for pixel classification

Potential function is an important concept of MRF. In different application environments, potential function usually has different definition form and that is the key to successful application. To achieve the aim of classifying the pixel between infrared target and background, the energy distribution difference between them discussed above should be utilized here in constructing the potential function.

$$V_c(x_s)=\frac{\hat{d}_{\tilde{\eta}_s^a}(x_s)}{\sqrt{\mathrm{var}(\tilde{\eta}_s^a)}} \tag{8}$$

where $\tilde{\eta}_s^a$ is the selected neighborhood which is the better characterization of the target area and var(·) is the variance function. The newly defined potential function $V_c(\cdot)$ describes the ratio of target energy and background and can help to make the Eq. (3) concise.

$$\begin{cases} x_s \text{ is target}, & \text{if } V_c(x_s)\geqslant T'_d \\ x_s \text{ is background}, & \text{if } V_c(x_s)<T'_d \end{cases} \tag{9}$$

where $T'_d=-\ln(Z\cdot T_d)$ is the new decision threshold. Generally, for the difficulty in calculating the partition function Z, the new threshold T'_d is also hard to estimate. But in this paper, the decision equation means the energy ratio of target and background, so some prior knowledge such as SCR (signal-to-clutter ratios) can be utilized in estimating the threshold.

2.4 Implementation

Let an unknown infrared image with targets scattered in it as the input image, (i,j) as the position of the pixel currently to be processed. The classification of the pixel should obey the following steps.

Step1: Respectively calculate the difference values $\hat{d}_{\eta_s^1}$, $\hat{d}_{\eta_s^{2a}}$, …, $\hat{d}_{\eta_s^{4d}}$, according to the Eq. (7) and neighborhoods η_s^1, η_s^{2a}, …, η_s^{4d}.

Step2: Select the just right neighborhood $\tilde{\eta}_s^a$, according to the maximum rule and difference values $\hat{d}_{\eta_s^1}$, $\hat{d}_{\eta_s^{2a}}$, …, $\hat{d}_{\eta_s^{4d}}$ calculated in Step1.

Step3: Calculate the potential function $V_c(x_s)$, according to the Eq. (8) and selected neighborhood $\tilde{\eta}_s^a$.

Step4: Set the decision threshold T'_d.

Step5: Classify current pixel according to the potential function $V_c(x_s)$ and decision threshold T'_d. If $V_c(x_s)\geqslant T'_d$, the pixel is classified as target and if $V_c(x_s)<T'_d$ as background.

Usually, there is some prior knowledge, such as signal-to-clutter ratios (SCR) *etc.*, while an image process system is designed. So the approximate rate between the energy of targets and backgrounds usually is known to the user of the process system, and that can be utilized in calculated the decision threshold T'_d. In this paper, the decision threshold is defined as $T'_d=k\cdot\mathrm{SCRs}$, where $k<1$ is a redundancy coefficient, represents some unknown factors that can make the reduction of the system's SCR in practice using. To say the least, if there is no prior information, the decision threshold T'_d can still be calculated through adaptive learning.

3 Experimental results

In this section, the performance of classic MRF model (CMRF) and extended MRF model with adaptive neighborhood systems (EMRF-AN) is compared. Firstly, three original short wave infrared images, as shown in Fig. 4 A_1, B_1 and C_1, are used. Secondly, these images are respectively added Gaussian random noises with zero means and targets with various radiation intensities and the pending images are generated as shown in Fig. 4 A_2, B_2 and C_2. Then, to make a comparison, the pending images are processed by separately using CMRF and EMRF-AN algorithms. The processing results are shown in Fig. 4 A_3, B_3, C_3 and A_4, B_4, C_4. The size of the images used in processing is 64×64, the designed SCR is 5 and the standard deviation (σ_{noise}) of the zero mean Gaussian noises

is 10. The minimum gray values of target areas ($\mu_{\min}$), means (μ_η) and standard deviations (σ_η) of the gray values of the selected neighborhood system and the final SCR are shown in Table 3, where $\mathrm{SCR}=(\mu_{\min}-\mu_\eta)/\sigma_\eta$. The software used in simulating is Matlab R2007a and hardware is a computer with Core 2@2.9 GHz CPU.

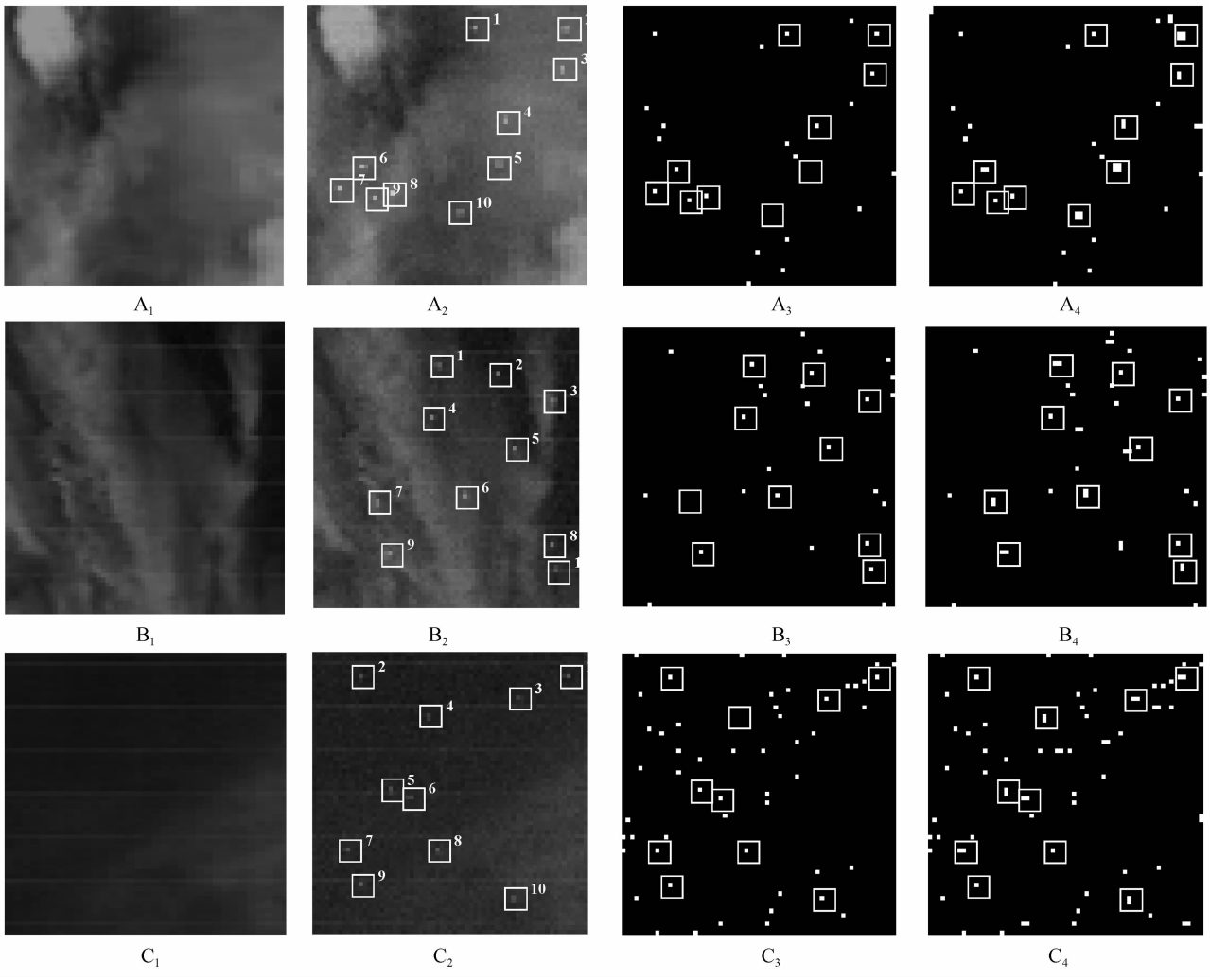

Fig. 4 Experiment results of two different algorithms(A_1, B_1, C_1 original background images; A_2, B_2, C_2 pending images including targets and noises; A_3, B_3, C_3 target detection results by CMRF; A_4, B_4, C_4 target detection results by EMRF-AN)

The simulation results in Fig. 4 show that compared with algorithms based on EMRF-AN, the algorithm based on CMRF will lose targets consisting of more than one pixel. By analysis, the reason is that the diffusion of target energy weakens target energy distributed on each pixel, and that the CMRF model cannot perfectly deal with this diffusing phenomenon and inconsiderately takes the pixels of targets as that of backgrounds, So the SCR finally decreases. That makes targets with shapes hard to be detected. For using the adaptive neighborhood system, the proposed EMRF-AN model selects the proper neighborhood system for each target and can seriously partition the pixels belonging to targets and backgrounds. So that the proposed algorithm has a stable performance.

To make a further experiment, two evaluation factors, target loss rate ρ and target area detection rate κ are introduced in the following.

$$\begin{cases}\rho=\dfrac{N^T_{\mathrm{Loss}}}{N^T_{\mathrm{Total}}}\\ \kappa=\dfrac{\sum_{m=1}^{N^T_{\mathrm{Det}}}A^D_m}{\sum_{n=1}^{N^T_{\mathrm{Total}}}A_n}\end{cases}\tag{10}$$

where N^T_{Loss}, N^T_{Det} and N^T_{Total} separately mean the number of lost, detected and total targets, the relations among them are $N^T_{\mathrm{Total}}=N^T_{\mathrm{Loss}}+N^T_{\mathrm{Det}}$. The symbols A^D_m and A_n separately mean the detected area and original area of the targets, in which the false targets are not included.

The values of ρ and κ, as show in Table 3, indicate that the proposed EMRF-AN algorithm has a higher target detection rates and better target

shape preservation performance.

Table 3　The SCR of targets

	Target No.		1	2	3	4	5	6	7	8	9	10	ρ	κ
A_2	CMRF	σ_η	7.8	12.6	15.1	11.1	**18.7**	12.3	5.6	6.0	4.7	**14.5**	0.2	0.38
		$\mu_{\min}$	147.3	140.9	160.4	159.8	**117.1**	175.0	181.7	203.5	173.9	**105.3**		
		μ_η	70.5	101.8	108.5	102.9	**93.2**	96.4	93.3	106.1	93.1	**77.5**		
		SCR	9.9	3.1	3.4	5.1	**1.3**	6.4	15.9	16.3	17.1	**1.9**		
	EMRF-AN	σ_η	7.8	3.5	2.7	3.7	**4.5**	4.6	5.6	6.0	4.7	**3.9**	0	0.95
		$\mu_{\min}$	147.3	106.7	145.3	129.0	**113.2**	126.4	181.7	203.5	173.9	**83.5**		
		μ_η	70.5	91.7	103.1	98.3	**83.2**	90.7	93.3	106.1	93.1	**66.8**		
		SCR	9.9	4.3	15.7	8.2	**6.7**	7.8	15.9	16.3	17.1	**4.3**		
B_2	CMRF	σ_η	10.5	5.5	13.8	5.5	7.7	8.8	**19.8**	3.8	12.2	9.6	0.1	0.47
		$\mu_{\min}$	88.9	105.2	116.3	120.2	120.3	134.9	**116.8**	109.6	135.2	82.6		
		μ_η	53.3	29.3	72.3	45.8	52.4	75.5	**79.9**	40.7	86.5	47.2		
		SCR	3.4	13.9	3.2	13.6	8.8	6.8	**1.9**	18.1	4.0	3.7		
	EMRF-AN	σ_η	6.9	5.5	13.8	5.5	7.7	4.7	**12.7**	3.8	7.3	6.5	0	0.79
		$\mu_{\min}$	72.3	105.2	116.3	120.2	120.3	94.5	**115.4**	109.6	109.9	65.0		
		μ_η	49.1	29.3	72.3	45.8	52.4	71.1	**75.5**	40.7	81.7	42.6		
		SCR	3.3	13.9	3.2	13.6	8.8	5.0	**3.2**	18.1	3.9	3.5		
C_2	CMRF	σ_η	7.0	6.9	5.6	**8.7**	9.8	9.1	5.8	7.0	3.5	7.9	0.1	0.45
		$\mu_{\min}$	84.8	74.4	62.7	**58.9**	74.2	68.7	77.8	84.0	92.8	75.5		
		μ_η	31.8	30.8	35.1	**33.7**	39.4	40.0	38.9	45.9	44.0	49.4		
		SCR	7.6	6.3	4.9	**2.9**	3.6	3.2	6.7	5.4	13.9	3.3		
	EMRF-AN	σ_η	2.9	6.9	3.2	**2.3**	5.1	2.8	3.0	7.0	3.5	4.3	0	0.85
		$\mu_{\min}$	47.2	74.4	46.1	**54.3**	59.8	61.9	51.6	84.0	92.8	67.8		
		μ_η	29.1	30.8	33.2	**30.9**	35.8	37.3	36.6	45.9	44.0	44.7		
		SCR	6.2	6.3	4.1	**10.2**	4.7	8.8	5.0	5.4	13.9	5.3		

4 Conclusion

Shape target detection under complex backgrounds is a challenge. In this paper, an adaptive neighborhood system was established by using the concluded target shapes as templates. Based on the adaptive neighborhood system, an algorithm using the MRF theory as foundation was proposed. In the proposed algorithm, a criteria function was constructed for the selection of the proper neighborhood and a difference operator was used for establishing the new potential function. The final experimental results verified that the proposed algorithm has a stable detection performance and can perfectly protect target shape details.

References

[1] TARTAKOVSKY A G, BROWN J. Adaptive spatial temporal filtering methods for clutter removal and target tracking[J]. *IEEE Transactions on Aerospace and Electronic Systems*, 2008, **44**(4): 1522-1537.

[2] LONG Yun-li, XU Hui, AN Wei, *et al*. Spatial temporal fused filtering for infrared clutter suppression based on restricted sequential M-estimation[J]. *Acta Aeronautica et Astronautica Sinica*, 2011, **32**(8): 1531-1541.

[3] ZAVERI M A, MERCHANT S N, DESAI U B. Tracking of point targets in IR image sequence using multiple model based particle filtering and MRF based data association[C]. IEEE Proceedings of the 17th International Conference on Pattern Recognition, 2004, 4: 729-732.

[4] PARAG T. Coupled label and intensity MRF models for IR target detection[C]. IEEE Computer Society Conference on Computer Vision and Pattern Recognition Workshops, 2011, 7-13.

[5] JIANG Y X, YUAN Q Z, SHAO C Y, *et al*. Study on detection method of small object on sea based on kernel-MRF foreground segmentation model[C]. IEEE Conference on Computer Science and Service System, 2012, 1869-1872.

[6] SUN X D, FANG G Z. Infrared small targets detection based on MRF model[J]. *Procedia Engineering*, 2012, **29**: 420-424.

[7] LI S Z. Markov random field modeling in image analysis[M]. Springer, 2009: 20-30.

[8] BESAG J. Spatial interaction and the statistical analysis of lattice systems[J]. *Journal of the Royal Statistical Society: Series B (Methodological)*, 1974, **36**(2): 192-236.

[9] ZHONG P, WANG R S. Image segmentation based on Markov random fields with adaptive neighborhood systems[J]. *Optical Engineering*, 2006, **45**(9): 097202.

[10] FORBES F, PEYRARD N. Hidden Markov random field model selection criteria based on mean field like approximations[J]. *IEEE Transactions on Pattern Analysis and Machine Intelligence*, 2003, **25**(9): 1089-1101.

[11] TZANNES A P, BROOKS D H. Detecting small moving objects using temporal hypothesis testing[J]. *IEEE Transactions on Aerospace and Electronic Systems*, 2002, **38**(2): 570-586.

[12] WANG Da-bao, LIU Shang-qian, KOU Xiao-ming, *et al*. Infrared background clutter suppression algorithm of adaptive regularization based on MRF[J]. *Journal of Infrared and Millimeter Waves*, 2009, **28**(6): 440-444.